Electrical transport in three-dimensional ensembles of silicon quantum dots

I. Balberg, J. Jedrzejewski, and E. Savir
The Racah Institute of Physics, The Hebrew University, Jerusalem IL-91904, Israel
(Received 8 April 2010; revised manuscript received 30 November 2010; published 24 January 2011)

Following our previous works in which we tried to understand the transport mechanisms below and at the conductivity percolation threshold of three-dimensional ensembles of Si quantum dots (QD's), in the present work we try to derive a comprehensive understanding of the transport mechanisms above the percolation threshold. Our conclusions are based on a systematic study of the electrical properties of Si nanocrystallite ensembles that are embedded in an insulating matrix as a function of their density. To evaluate the transport mechanisms we introduce the concept of "touching," showing that its application enables to suggest that the percolation transition is associated with the onset of extended states-like transport in a continuous disordered network. This understanding provides a framework for the discussion of the transport in ensembles of QD's in general and in ensembles of Si QD's in particular.

DOI: 10.1103/PhysRevB.83.035318 PACS number(s): 73.63.−b, 72.20.Jv, 73.23.Hk, 74.62.Bf

I. INTRODUCTION

In contrast with the optical properties that have been studied intensively,[1] the understanding of the transport in solid ensembles of semiconductor quantum dots (QD's) is still at a very rudimentary level.[2] The purpose of this paper is to lay a foundation for the discussion of the transport in such systems by considering the corresponding phenomena in a system on which few data already exist, but for which a critical discussion of the transport has not been given yet. This is the system of Si nanocrystallites (NC's) that are embedded in an insulating matrix.[3,4] The interest in the transport in this system is expected to follow the new basic physics that it reveals and the potential applications that it suggests.[3,5] In particular, we expect that, in addition to the reasonable (though still controversial[6]) understanding of granular metals[7,8] and conventional semiconductors,[9] new significant insights as to the transport mechanism and related phenomena in ensembles of semiconductor QD's will be found. For example, the combination of Coulomb blockade (CB) and quantum confinement (QC) restrictions can yield various resonant tunneling effects[10] as well as various quantum phase transformations.[11] Considering applications, we note charge storage memories,[5] solar cells,[12] and light emitting diodes.[13] In the latter case one realizes that significant electroluminescence (EL) can come about only in dense enough three-dimensional (3D) ensembles of semiconductor NC's.[13–15]

Being concerned with the transport in 3D ensembles of Si QD's it is apparent that the understanding of the electronic structure[16–18] and the electrical properties[19,20] of the single isolated NC[15] is quite necessary to interpret the transport data in ensembles[21–23] of semiconductor NC's. Noting, however, that reviews on the electrical properties of essentially isolated NC's are available,[5,15] we mention here only that such systems have a well-defined double barrier tunnel junction (DBTJ)-like configuration that is reminiscent of the DBTJ's that were studied in the II-VI and III-V NC's.[19,20] On the other hand, the above studies of "isolated" Si NC's,[15] while providing convincing evidence for the effect of CB on the transport, did not provide conclusive evidence for a role of the quantum confinement effects (i.e., resonant tunneling) on the transport.[24]

In contrast with the lower-dimension ensembles,[5,15] the electrical transport in denser ensembles of 3D systems of Si NC's has not been studied intensively. It appears to us that the foremost conspicuous drawbacks in the majority of the corresponding previous studies were the lack of correlation between the geometrical structures of the ensembles and/or the density of the NC's N in them, on the one hand, and the nonconclusive interpretation of the transport data, on the other hand. In fact, usually, a single macroscopic transport measurement on such ensembles was interpreted as due to a particular transport mechanism that may or may not be consistent with the structure of these ensembles. Also, in the majority of the studies, the transport mechanism was deduced essentially only from the temperature dependence of the dark conductivity $\sigma(T)$. Due to the relatively high resistance of the samples, the temperature range over which it was possible to carry out the measurements was relatively narrow, and thus the analyses presented cannot be considered conclusive. The combination of the above drawbacks tempted many researchers to suggest that the transport mechanism in their samples is "hopping," without even specifying whether the hopping is between the NC's or between some other entities, such as defects in the system.[15] Obviously, without knowing the value of N this assignment is not meaningful. Also, the mechanism of thermionic emission[25] has been usually suggested for systems where N was *a priori* assumed to be very high.[26,27] The fact that the suggested semiconductor barriers have little meaning (there is, on the average, only a single free electron per NC) has been ignored in these works. Correspondingly, even in recent reviews[15] no attention was given to the importance of the density of the NC's, and the $\sigma(T)$ dependence was suggested to represent unspecified tunneling processes at low temperatures and a thermionic emission process at high temperatures. One must conclude then that the very popular $\sigma(T)$ data by themselves may yield questionable interpretations. In fact, as discussed in the present paper this applies also for the other popular measurement, that is, that of the current voltage (I-V) characteristics for which the derived I(V) dependence and its interpretation are not unique.

Following the previous considerations, we attempt to present here probably the first critical report of the transport in relatively dense ensembles of Si NC's embedded in insulating continuous matrices, adding [to the very common study of the σ(T) and I-V dependencies] the very important information on the density of the NC's. In particular, the latter consideration also adds the important system-connectivity aspect of the transport that has hardly been discussed in the past. This is in contrast with the interdot tunneling aspect that was emphasized more frequently. We note, however, that the need to consider the connectivity as well as the intercrystallite charge transfer was first recognized by Burr *et al.* in 1997[14] while the first specification of the density of such ensembles was given by Fuji *et al.* in 1998[21] for ensembles of Ge NC's. As we discuss in this paper, other works on the transport in Si or Ge NC's ensembles did not yield conclusive σ(T) or I-V dependencies, thus leaving the problem of transport in relatively dense 3D systems of Si QD's quite unresolved. Correspondingly, we try in this work to gain a comprehensive understanding of the previous transport studies by considering these dependencies as a function of the density of the NC's. In particular, deriving the concept of NC's "touching" gives us here a key for the analysis of the various transport data beyond the very dilute NC's range where granular-metal-like hopping conduction[6–8,28,29] is probably the only possible transport mechanism. For the achievement of the above understanding we have studied well-characterized structures of Si-NC's ensembles and we have carried out the popular σ(T) and I-V measurements on a variety of related and less related structures. All this was to reduce the number of the possible mechanisms that can account for the experimental data.

The present paper is structured as follows. In Sec. II we present our method of sample fabrication that enabled us to carry out a systematic and comprehensive study of the electrical properties as a function of the density of the NC's. Then we describe the structural and electrical measurements that we performed to appreciate the combined effects of inter-NC's conduction and the connectivity of the system on the transport mechanisms. In Sec. III, we present our experimental results that emphasize the great importance of knowing the structure of the 3D system and of combining it with the transport data for which we provide results and analyses that were not presented yet in the literature. We believe then that, as summarized in Sec. IV, our results and their interpretation provide an initial framework for the discussion of the transport mechanisms in 3D ensembles of Si NC's.

II. SAMPLE PREPARATION AND MEASUREMENT TECHNIQUES

Focusing in this study on the transport in relatively thick films of Si/SiO_2 nanocomposites and emphasizing here the effect of the NC's density on the transport properties we have applied[30,31] probably the most suitable sample preparation method for such studies (i.e, the cosputtering technique that is well reviewed in the literature).[7,8] This is because the flexibility of this method provides a *very wide scale of nanoparticles densities that are fabricated under exactly the same conditions*.[32] We note that while many groups have used the sputtering technique for the deposition of Si/SiO_2 films and some[21] have applied it for obtaining a few Si phase contents, we do not know of any other group that applied this technique for obtaining such films with a continuous NC's density as a parameter. Using this versatility is the experimental basis for the present work that enabled us to carry out a systematic study of the electrical properties as a function of the NC's density in a manner that has been previously applied only to granular metals.[7,8,33]

In the present work we have cosputtered the studied films by utilizing two separate sources (targets), 5 cm in diameter each, with their centers 10-cm apart. One target was of a high purity (99.999%) sintered silicon pellet or electronic quality crystalline Si wafer, while the other consisted of pure (99.995%) fused quartz. The Si wafers (when used) were *n*-type crystals with resistivities of 0.005, 0.1–0.5, and 20–30 Ω cm, and *p*-type crystals with resistivities of 0.015 and 20–30 Ω cm. These targets have been used in the studies of the doping effects on the electrical properties of the Si/SiO_2 system. The substrates that we used were 13-cm long, 1-cm wide, and 0.7-mm thick quartz slides. For the sputtering process the substrate was positioned above the line connecting the centers of the two targets and parallel to it.[34,35] The deposition conditions in our studies were not too different from those used in the deposition of granular metal films[7,8,33] and in other works on Si/SiO_2 composites.[36]

As pointed out previously, the main key to the understanding of the Si NC's system in the present study is the ability to have sets of Si NC's ensembles with continuous variations of their concentration[34,37] and the NC's size.[37–39] In general, following a couple of hours of deposition, the substrate became coated with a film that was about 1-μm thick. The film so prepared is a mixture of Si and SiO_2, and since these two phases are immiscible a composite of the two phases forms. The film was Si-phase rich at one end of the elongated substrate (the one close to the Si target) and SiO_2 rich at its other end.[30,31,37–41] Our Raman scattering, infrared (IR) spectroscopy and x-ray diffraction (XRD) measurements confirmed that our films consist of amorphous SiO_2 and amorphous silicon (a-Si). For finding the relative volume contents of the two phases along the cosputtered film we have applied the very common (film thickness measuring) procedure for the finding of the metallic volume content in granular metals.[7,8,32] We[34] and others[36] found, in particular by IR spectroscopy, that this procedure is amenable for the determination of the content of the SiO_2 phase as well as the fractional volume% content of the Si phase x. The latter quantity, which is the ratio of the volume of the Si (amorphous or crystalline) phase to the volume of the film (that consists of the Si phase and the SiO_2 phase), given as vol.%, will be our NC's density characterization parameter throughout this study. In our study we have monitored then the variation of the various properties as a function of the position along the substrate and this was translated to the dependence on the value of x.

In order for the a-Si phase in the as deposited films to crystallize the films were annealed (at 1150–1200 C for a typical duration of 40 min, under a flow of 4 litre/min of pure N_2). After annealing we reapplied the previous structural characterization methods and added to them high-resolution transmission electron-microscopy (HRTEM) measurements.[37,38]

This characterization revealed that, while some small amounts of silicon NC's were found (by Raman scattering) in the nonannealed a-Si/SiO_2 samples, no a-Si was detected in the annealed samples which were found to consist of Si NC's and amorphous SiO_2. For the latter samples knowing the NC's size dependence on x[38] we have also determined the density of the NC's, $N = 6(x/100)/(\pi d^3)$, where d is the diameter of the crystallite. In particular, we found typical diameters, around 3 nm, at the Si poor end of the film, and diameters around 10 nm at the Si rich end of the film.[37–39]

To be able to carry out the electrical measurements we have provided electrical contacts by sputtering aluminum or silver electrodes, 1-mm wide (0.2 to 1 μm thick) with a 1-mm separation between two adjacent ones.[30,31,41] We have carried out then standard four-probe conductivity σ and photoconductivity σ_{ph} measurements,[30,31] and we obtained current voltage (I-V) and current-time (I-t) characteristics. The above electrodes separation enabled us quite an accurate mapping of the dependence of the above-mentioned properties on x, with a resolution of $\Delta x \approx 2$ vol.%.

For finding the local current routes in the samples we have applied our conductive AFM (C-AFM) technique.[41,42] These measurements were taken both in the dark and under illumination. The information obtained enabled us then to evaluate whether a suggested transport mechanism (the derivation of which is based on macroscopic measurements) is consistent with the observed current paths.[42] We note that this precaution, of carrying out simultaneously such microscopic and macroscopic measurements of the global transport of the 3D systems of Si NC's, has not been taken before, thus leaving always some uncertainty regarding the suggested transport mechanisms.

In our study we have derived the I-V and I-t characteristics by applying a voltage to the sample and determining the current by measuring the voltage drop across a small in-series resistor. For the photoconductivity a He-Ne laser (633 nm with a flux of 70 mW/cm^2)[30,31] or a solid-state laser (473 nm with a flux of 250 mW/cm^2)[41] were applied. The difference between the current under illumination and in the dark was taken to be the photocurrent through the sample from which the value of the photoconductivity σ_{ph} was derived. As we show in the following, the comparison of σ and σ_{ph} has provided further information regarding the transport mechanisms. In particular, we note the very informative nature of the light intensity exponent of the photocurrent γ_e $(=\mathrm{d}[\ln(\sigma_{ph})]/\mathrm{d}[\ln(G)]$, where G is the charge carriers generation rate that is determined by the flux of the impinging illumination).[43,44] Here γ_e was determined over the range of 2–70 mW/cm^2. All these transport measurements were carried out in the room-temperature-liquid-nitrogen temperature range by utilizing a cryostat with a temperature controller.

In view of the wide interest in the optical properties of Si-NC's systems[37,40] our standard characterization tool of the samples was the x dependence of their spectral photoluminescence (PL),[30,31,37–40] absorption, and ellipsometry,[45] as described in great detail previously.

III. RESULTS AND ANALYSIS

Following the importance that we attribute to the NC's density as a guide for the evaluation of the transport mechanisms in ensembles of QD's and following the description of how this density was derived, we start this section by mentioning the typical x dependence that we found for the conductivity $\sigma(x)$. This behavior is characterized by the fact that up to about a critical value x_c the results simply reflect the background conductivity of the experimental system and thus we cannot draw any direct conclusions regarding the transport mechanism. On the other hand, as x increases above x_c, we find a strong rise in the conductivity that can be well fitted to the prediction of percolation theory[46–50] that $\sigma \propto (x\text{-}x_c)^t$, where x_c is the percolation threshold and t is a constant. For lattices and continuum systems, the latter value (in 3D) is expected[46–49] to be equal or larger than the universal-dimensional value of $t_0 \approx 2$.[30] Measurements on tens of samples that we prepared under basically similar, but not exactly identical conditions have revealed x_c values in the range $30 \leqslant x_c \leqslant 40$ vol.% and t values in the range $2 < t < 4$ for the annealed samples, and $25 \leqslant x_c \leqslant 35$ vol.% and $2 < t < 5$ values for the nonannealed samples. We note in passing that typically for a given sample we have determined the value of x_c within ± 1 vol.% and the value of t within ± 0.2.[30] One should note, however, that in the present study the very exact values of these parameters are not essential since in the comparisons that will be made between different samples we will be concerned only with trends that are associated with the proximity to the percolation threshold. Correspondingly, the scale that we will use then for the comparisons will be x/x_c. The trends to be discussed were found to be robust throughout the tens of samples that have been examined. We note also, in particular, that the value of x/x_c determines the connectivity of the system[47,49] on the one hand[47,49] and the importance of charging[30,31] effects on the other hand. Following that we also use the corresponding x_c value *as a prime reference point for* x in the discussion presented in this paper. In passing we note that we found previously that both $\sigma(x)$ and $\sigma_{ph}(x)$ have the same $\sigma(x)$ dependence indicating that this dependence is associated with the connectivity of the system under study.[30,50]

In what follows we will examine then the electrical characteristics of the system for $x \geqslant x_c$.

To set the stage for the description of our samples we show in Fig. 1 the structure of the system just below x_c. In this HRTEM image we see some geometrically isolated crystallites (that may have a small distortion from sphericity), the presence of "touching" pairs and the further distortion of the NC's in regions of relatively high NC's densities (so as to accommodate the crystallites that are grown in their proximity). For a more precise and visual definition of the concept of "touching," let us consider the NC's 1 and 2 as "touching" while we call NC 3 a "geometrically isolated" or a "nontouching" NC. We define then, here, two NC's as "touching" if the distance between their surfaces does not exceed the order of a lattice constant ($\approx$0.5 nm in Si). In passing, we note that only the well-known hopping process[48,51] can be the transport mechanism between nontouching NC's.

Considering the structure of the high-x ($x > x_c$) regime we see in the HRTEM image of Fig. 2 that in this regime there is

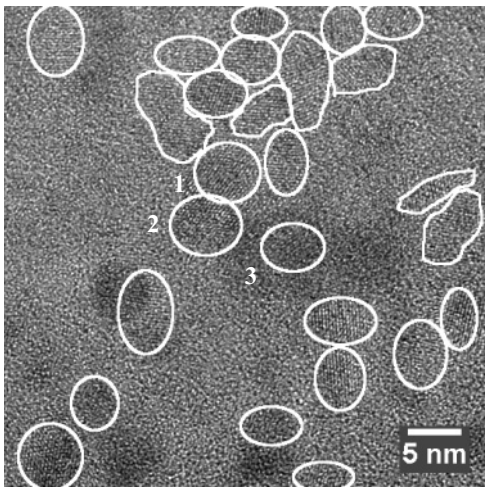

FIG. 1. A HRTEM micrograph of a sample of our annealed cosputtered films with 25 vol.% of Si phase content. The crystallites, identified by their Si lattice fringes, are marked by their borders. One notes that with the increase of density the crystallites grow and change from a spherical shape to shapes that can accommodate their density. The two NC's, 1 and 2, are defined as "touching" while NC 3 is defined as a geometrically isolated NC. Note that the increase of x causes "more and more" NC's to "touch" their neighbors.

a further growth of the individual NC's, further distortion of the crystallites, and most importantly, the apparent presence of very large clusters of "touching" NC's. Note that while it is not obvious from the two-dimensional HRTEM images, we do have here a 3D network of connected "touching" crystallites. To confirm that the latter applies also to the current paths, and to show that in our study the macroscopically measured currents pass through the NC's and not via possible bypassing paths (such as a possible residual a-Si network that may still be present in the sample) we have carried out C-AFM measurements on samples for which the

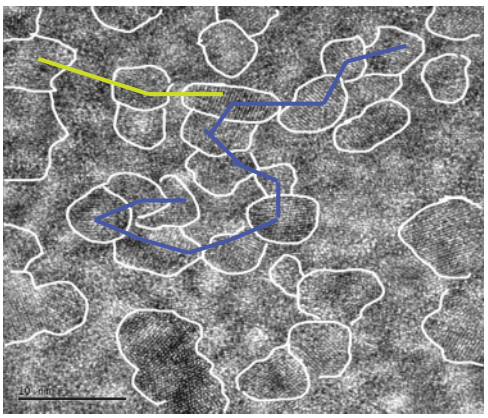

FIG. 2. (Color online) A HRTEM micrograph of our annealed cosputtered film with 80 vol.% Si phase content. A continuous network of "touching" NC's is seen to be formed. A typical continuous current path is illustrated by the dark (blue) segments on the micrograph. A possible tunneling current path via a DBTJ-like configuration is marked by the light (yellow) segments in the micrograph.

macroscopic conductivity has been measured simultaneously. Indeed, we have found that the current flows through the NC's.[41] Following these findings we illustrate by a dark (blue) track in Fig. 2 an expected percolation current path which indicates the existence of a global 3D percolation conductance via "touching" NC's. The possible conduction via isolated (nontouching) NC's, as indicated by the bright (yellow) segments in the figure, will be discussed later. The structure we observe in Fig. 2 is reminiscent of the structures that were observed in three other systems, for which, unlike the present system, the transport has been studied by us and by others extensively and with which we will compare our results. These are granular metals,[7,8,49,52] hydrogenated microcrystalline silicon (μc-Si:H),[42,53] polycrystalline silicon, and semi-insulating polycrystalline silicon (SIPOS).[25,54–56]

Turning to the transport measurements, we note that one does usually learn on the transport mechanism by measuring the conductivity as a function of external parameters, the most common of which are the temperature and the applied voltage.[51] However, before summarizing the data that we obtained, let us point out the difficulties associated with the nonuniqueness of the possible interpretation of the temperature and/or the applied voltage dependencies of the conductivity. In particular, we will show that these dependencies by themselves cannot distinguish reliably between different mechanisms. Rather, a comparative study of these and other dependencies in various systems, such as done in the present study, enables to narrow down substantially the number of possible transport mechanisms that were or may be suggested for ensembles of Si NC's in the regime under study.

Following the latter consideration we show in Fig. 3 typical σ(T) and σ_{ph}(T) data that we obtained for a sample of $x \approx$ 67 vol.% (where for the corresponding cosputtered film the value of x_c was 31 vol.%). We start, in Fig. 3(a), with the most common presentation of such data (i.e., as a $\log_{10}\sigma$ versus 1000/T plot). Trying to fit these results by an Arrhenius plot, $\sigma = \sigma_A \exp[-(T_A/T)]$, where, σ_A and T_A are constants of the system, we see that the data cannot be accounted for by a single activation energy value E_a ($= kT_A$), for the entire temperature range. On the other hand, a best fit that corresponds to such an activated process can be obtained (solid curve) by considering $\sigma = \sigma_1 + \sigma_2$, where σ_1 is the asymptote to the σ(T) data at the low temperature end and σ_2 is the asymptote to the σ(T) data at the high temperature end of the above range. The excellent fit obtained suggests that we have either two processes that are activated in parallel (such that σ_1 is dominant at low temperature and σ_2 is dominant at high temperature) or that we have a process that is composed of a series of excitations, the activation energies of which are distributed between the corresponding two extremes, E_{a1} and E_{a2}. It will be important for our discussion in the following to note that the behavior shown in Fig. 3(a) is typical of many homogeneous ordered[9] or disordered[57–60] systems. We also see in Fig. 3(a) that σ_{ph}(T) has a milder variation with temperature than σ(T) throughout the entire temperature range. This is rather a general feature of photoconductivity in semiconductors in general,[43] and in disordered Si systems in particular.[61] The latter behavior is explained by the shift of the demarcation level (at which the trapping rate equals the recombination rate) toward the Fermi level E_F, with increasing temperature.[43] In turn, this σ_{ph}(T)

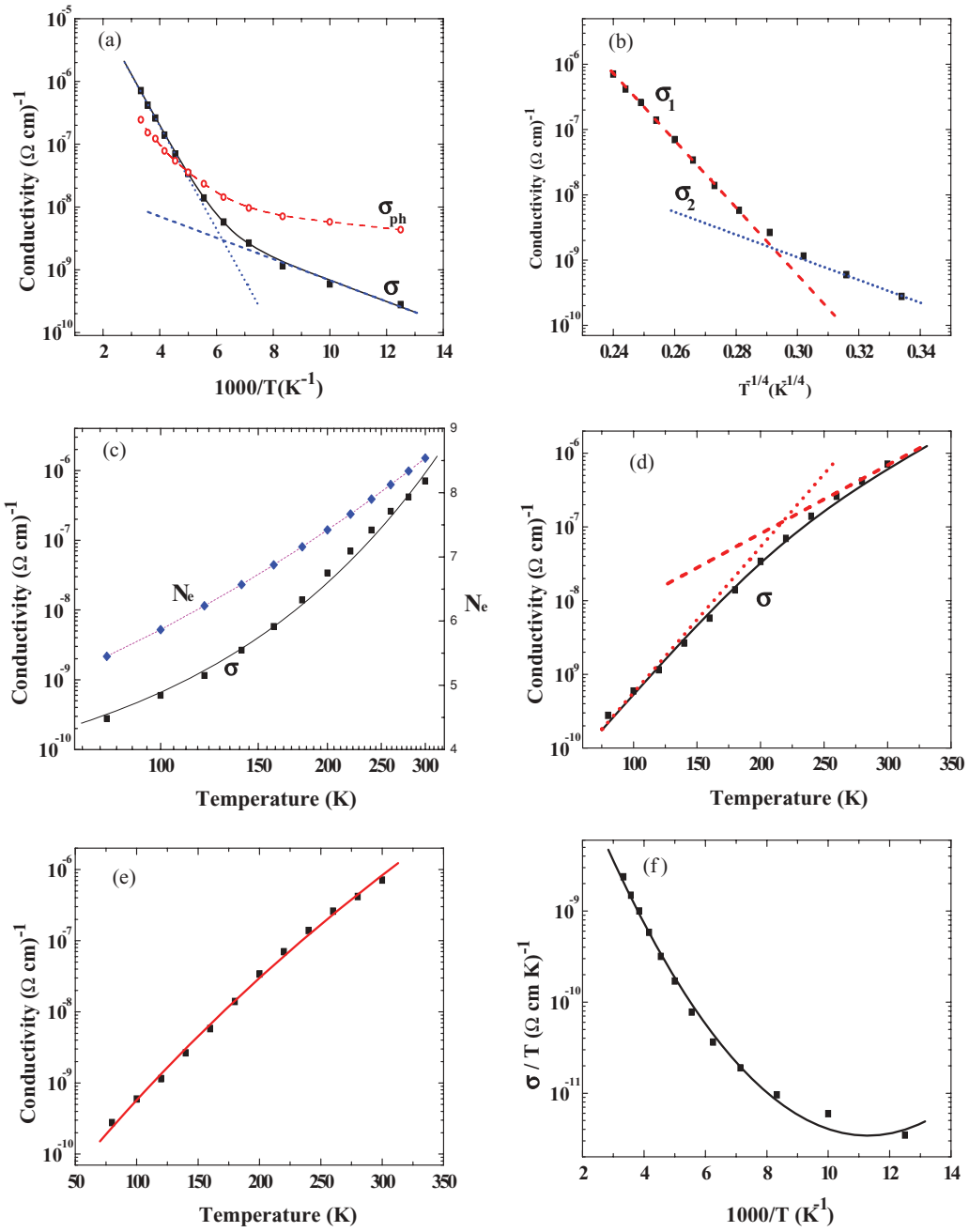

FIG. 3. (Color online) The temperature dependencies of the conductivity σ and the photoconductivity σ_{ph} (a), measured at V = 40 V, in the high-x ($\approx 67 > x_c = 31$ vol.%) regime. The same data are fitted by various dependencies that were suggested for transport mechanisms in the literature. (a) A single Arrhenius plot cannot fit the entire data but the same data can be well fitted (σ) by a parallel addition ($\sigma_1 + \sigma_2$) of two such plots. (b) A single "Mott $T^{-1/4}$" dependence cannot account for the entire data, but again, two such plots can account for them. (c) The concave behavior of the σ data can be hardly fitted by a single Berthelot dependence. Assuming that the data can be fitted to a $\sigma \propto T^{\delta}$ dependence with a temperature-dependent $\delta = N_e\text{-}2/(N_e+1)$, yields the N_e values that are shown in this figure. (d) The σ data can be well fitted by a series combination (i.e., $\sigma^{-1} = \sigma_1^{-1} + \sigma_2^{-1}$) of two Berthelot dependencies. The data are also well accounted for by (e) the "$T_1/(T + T_2)$" dependence and by (f) the "$a\text{-}b/T + c/T^2$" dependence.

behavior may indicate a *continuous distribution* in energy of the trapping-recombination centers between the conduction band edge E_c and E_F. Since the previous two features (i.e., the nonsingle activation energy and the milder variation of the photoconductivity) are general features *of all the many measurements that we carried out we will not show more of them* but we will stress the self-consistent interpretation of these features and the correlation between the quantities that are derived from them [such as $\sigma(T = 300\ K)$ and $E_a(T = 300\ K)$, or $\sigma_{ph}(T = 300\ K)$ and $\gamma_e(T)$] and the structural data shown in Fig. 2. However, before discussing the dependence shown in Fig. 3(a) in more detail let us evaluate the data exhibited there in light of the other possible transport models that may account for them. For brevity, we will not

review the parameters derived in the corresponding fits to the prediction of the models, but rather concentrate on the functional dependences associated with them.

Our next step will be to fit the above $\sigma(T)$ data to a hopping-type dependence of the form $\sigma = \sigma_H \exp[-(T_H/T)^{\gamma}]$, where, σ_H, T_H, and γ are constants of the system. As with the earlier Arrhenius presentation we did not find any single T_H value, for any particular $\frac{1}{4} < \gamma < 1$ value that can account for the entire data. This is illustrated in Fig. 3(b) by the inability to fit the entire data by a single linear dependence. On the other hand, as shown in Fig. 3(b) with two T_H and/or two γ values, the two $\sigma(T)$ dependencies can be added to yield a good fit to a $\sigma = \sigma_1 + \sigma_2$ dependence with the same or different γ values in the two regimes. However, as was pointed out by many authors before[62] (but still ignored by many others), over the temperature range studied here (and, of course, when only part of it is utilized),[63] it is rather difficult to distinguish reliably between fits with different γ values (in the $1/4 \leqslant \gamma \leqslant 1$ range). In other words, the derivation of a γ value from data such as ours (with no other supporting evidence or without assuming *a priori* a given model) cannot be considered as good enough for establishing reliably a conduction mechanism. For example, a behavior with $\gamma = 1/2$ (or $\gamma = 1/4$) that was attributed by some authors[63] to a hopping-like conduction between the crystallites has not been conclusively supported by other evidence. It appears then that for the hopping-like models the suggestions that were based solely on the $\sigma(T)$ data[15] for single x values do not meet the criterion of an additional test.

The two $\sigma(T)$ dependences that we mentioned previously yield a convex $\log_{10}\sigma$ versus $\log_{10}T$ behavior. The fact that we cannot fit our data with a single T_A, T_H, and γ dependence suggests then that our data may yield a concave $\log_{10}\sigma$ versus $\log_{10}T$ behavior. Indeed presenting the data in such a plot in Fig. 3(c) shows such a behavior. In view of that we turned to fit the data to a single Berthelot dependence[64–70] $\sigma = \sigma_B \exp[(T/T_B)]$, which has the concave $\log_{10}\sigma$ versus $\log_{10}T$ behavior. Here σ_B and T_B are the appropriate parameters of the system. This much less abundant and much less understood dependence has been reported for some semiconductor[65–67] and some nanosemiconductor[68,69] systems, and it was interpreted to be associated with thermally activated tunneling via a barrier. The observed resultant behavior was suggested in the latter models to be due to the competition between the needed thermal excitation energy and the width of the barrier; the higher the temperature the larger the number of carriers that can tunnel through the narrower part of the barrier, such that the maximum tunneling probability yields the Berthelot-like behavior.[69] As shown in Fig. 3(c), while the Berthelot fit is not accurate it may be considered as "reasonable." On the other hand, assuming a series connection of two resistors, with two different T_B values, the Berthelot-dependence yields, as seen in Fig. 3(d), an excellent fit to a $\sigma^{-1} = \sigma_1^{-1} + \sigma_2^{-1}$ dependence. Such a dependence was suggested, for a very different system, by Fisher *et al.*[70] who interpreted their data in light of the barrier fluctuation model. In that model, for narrow tunneling junctions, large, thermally activated voltage fluctuations are induced. These cause then an increase of the tunneling probability as the temperature is increased. The σ_1 and σ_2 that they used were the Berthelot asymptotes at the high and low ranges of temperature. Within the same framework of similar models[70,71] one can well fit the data to a single $\sigma(T)$ dependence by utilizing the function $\sigma \propto \exp[-T_1/(T+T_2)]$ as suggested by Sheng *et al.*,[72] where T_1 and T_2 are system parameters. Such a fit is shown in Fig. 3(e). Another barrier-type model that was suggested by Werner[73] is based on thermionic emission but under the assumption that there is a given fixed-in-time Gaussian distribution of the barrier heights between the crystallites. This model yields that $\sigma/T \propto \exp(a\text{-}b/T+c/T^2)$ where, a, b, and c are constants. As seen in Fig. 3(f), in this kind of fit the "parabolic contribution" to the "left branch" of the parabola enables the "flexibility" that brings about a relatively good fit to the data. We note though that in the last two fits there are more parameters than in the previous simpler fits and thus the improved fitting does not necessarily indicate the applicability of the suggested mechanism. It also turns out that the behavior exhibited in Fig. 3(c) can be attributed to a variable range hopping (VRH)-like model.[74,75] In particular, one notes that in VRH the hopping range decreases and thus the number of hops in a given transport path N_e increases with increasing temperature.[48,51,60] In that hopping model $\sigma = \sigma_0 T^{\delta}$ where $\delta = N_e\text{–}2/(N_e+1)$. The basic physics of this process is that, in contrast with the above local barrier and hopping models, we have here a network effect that is actually associated with a one-dimensional (1D)-like conduction path rather than a 3D-like conduction network. Trying to fit our data to this model we determined [from Fig. 3(c)] the slope δ and derived from it the "expected number" of hops N_e according to the above relation. As seen in this figure, N_e changes between 5 and 9 over the studied temperature interval. We note though that in works on rather homogeneous systems,[75,76] which are much smaller than our 1 mm contact separation, the typical N_e values were also in the $1 \leqslant N_e \leqslant 12$ range. Hence, again, the good fit cannot make *a priori* the corresponding mechanism more plausible than all the mechanisms discussed previously. In contrast, arguments as given above or a comparative study, as we report in the following, can narrow down the number of mechanisms that properly account for the system under study.

Turning then to the I-V characteristics one should note that one has to apply the same caution that we have suggested in the consideration of the $\sigma(T)$ dependencies. For example, in Fig. 4 we show the I-V characteristic of a typical sample ($x \approx 50$ vol.%) by presenting it on a $\log_{10}I$ versus V (a) and a $\log_{10}I$ versus $\log_{10}V$ (b) scales. The first presentation of the same data shows an excellent fit to an $I \propto \sinh \kappa V$ dependence (where κ is a constant) that corresponds to one of the barrier models[70] that we mentioned above. The other presentation of the same data suggests a change of the logarithmic slope from 1.12 to 1.85 that is typical of the transition to a space charge limited current[9,14,43] behavior. Similar considerations apply to a Foweler-Nordheim tunneling dependence[9] but this mechanism seems *a priori* inapplicable here since our applied voltage is dropping along many barriers (or junctions) and we expect to get, as in tunneling characteristics for low applied bias, a linear I-V dependence. Hence, when linear, the linearity of the I-V characteristics may hide the actual behavior that the theories predict for a single barrier or junction. We see then that concluding a mechanism solely on the basis of such I-V fits

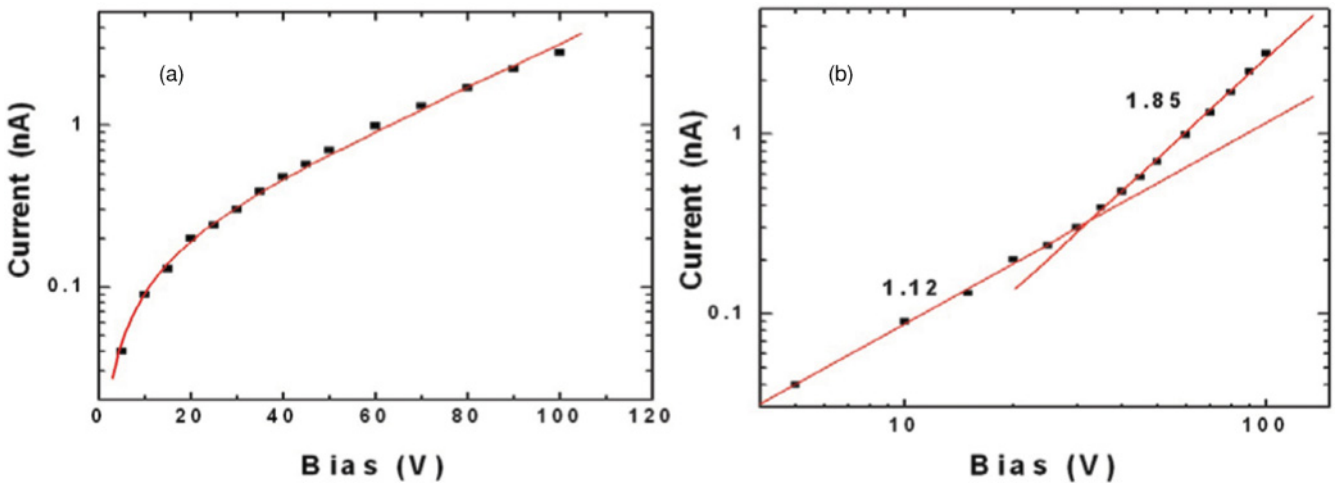

FIG. 4. (Color online) Typical room temperature I-V characteristics for $x = 50$ vol.% sample (where $x_c = 31$ vol.%). The data are fitted by (a) an $I \propto \sinh\kappa V$ dependence, and by (b) two segments of a power-law dependence, with exponents as given in the figure.

has the same drawbacks that we encountered in the attempts to draw conclusions solely on the basis of the $\sigma(T)$ behaviors.

As we tried to convey in this paper, even the combination of both the $\sigma(T)$ and the I-V dependencies cannot yield a unique determination of the transport mechanism. However, as most of the previous interpretations are associated with transport through potential barriers we turned to experimentally evaluate the corresponding mechanisms more thoroughly by depositing pairs of samples such that in some of them the presence of barriers is unlikely to exist (e.g., in nonannealed a-Si samples) while in others (such as seen in Fig. 2) they may exist between "touching" crystallites. We have compared then the $\sigma(T)$ and I-V dependences on such pairs of samples. In the sample pairs that we prepared one sample was an as-sputtered (i.e., not annealed) film and the other followed our annealing procedure as described in Sec. II. As the results of the $\sigma(T)$ behaviors were found to be similar for similarly fabricated samples we will only summarize here the general trends of the data and give only a couple of conspicuous examples for demonstration of these trends. In particular, these examples show that the effects in the trends are significantly larger than the error bars in the measured parameters.

The most general conclusion that we derived from our experimental results on the *tens of samples* that we have examined (sputtered, cosputtered, doped, and undoped) was that for the nonannealed samples, the I-V characteristics were linear for any value of x. This is in sharp contrast with the annealed samples where the I-V's became nonlinear when the percolation threshold was approached. In particular, these findings are consistent with a continuous a-Si network in the nonannealed case and with the existence of DBTJ's in the vicinity of x_c in the annealed samples.[30] Turning to the $\sigma(T)$ data we found that in all the studied samples the qualitative behavior was similar to that shown in Fig. 3(a). Correspondingly, we tried to follow the trends of the room temperature dependence of E_a in the different samples and their dependence on the proximity to x_c.

Starting with the sputtered, Si-only samples (where "what varies" with x is just the thickness of the Si film), we found that for the nonannealed samples the E_a values were in the range 0.23–0.29 eV for different samples or for different x values on the same sample. No systematic dependence on x was found there within a given sample. The results on the annealed samples were quite the same with somewhat lower E_a values that were in the 0.22 to 0.24 eV range. In other words, the crystallization did not change considerably the value of E_a, even though the conductivity has changed by about two orders of magnitude. In contrast, in the cosputtered films (i.e., in the Si/SiO_2 composite) we found, for example, that for the nonannealed samples E_a increased from 0.10 eV (for $x/x_c = 1.75$) to 0.15 eV (for $x/x_c = 1.15$), while for the annealed samples E_a increased from 0.17 eV (for $x/x_c = 1.59$) to 0.26 eV (for $x/x_c = 1.15$). The conspicuous result is then that in the Si/SiO_2 films there is a clear and substantial decrease of the E_a values in comparison with those in the Si-only films, on the one hand, but a substantial increase of E_a as the percolation threshold is approached, on the other hand. The latter increase is strongly enhanced in the annealed samples. In all the above E_a values the experimental uncertainty in their values was less than ± 0.03 eV and thus *the important point to stress is that the uncertainty in the E_a values is smaller than the variation between the E_a values of the annealed and nonannealed samples, or the variation of these values with x.* Combining these observations with the above mentioned behavior of the I-V characteristics we conclude that the properties of the Si/SiO_2 systems are only quantitatively different from those of the a-Si-only systems for $x \gg x_c$ (probably due to oxygen doping, see below) but there is a conspicuous difference between them as x_c is approached. This difference that is manifested by the systematic increase of E_a with the decrease of x/x_c in the former systems, as discussed in the following, is associated with the pronounced charging effects when $x \approx x_c$.

To further establish the previous conclusion we carried out also a comprehensive study of five doped samples where in the cosputtering process the Si source was an n-type Si wafer with a resistivity of 0.005 Ω cm (see Sec. II) that is expected

to have a concentration of 10^{18} cm^{-3} donors.[77] This was, of course, because the higher conductivity of the system enabled us then to approach more closely the vicinity of x_c. Here, for the nonannealed samples we found, for example, that E_a increased from $E_a = 0.095$ eV (at $x/x_c = 1.65$) to 0.14 eV (at $x/x_c = 1.23$) and 0.16 eV (at $x/x_c = 1.10$), while for the annealed samples we found that E_a increased from $E_a = 0.10$ eV (at $x/x_c = 1.65$) to 0.23 eV (at $x/x_c = 1.25$) and 0.35 eV (at $x/x_c = 1.05$). These latter results emphasize then that for x removed from x_c the thermal excitations in the two systems (annealed and nonannealed) are roughly similar but they differ considerably when x approaches x_c.

Combining all the previous results, for x well above x_c, with the corresponding general observation of linear I-V's for the nonannealed samples[30] and (above the vicinity of x_c) for the annealed samples, it appears that all these systems, for $x \gg x_c$, are very similar as far as the origin of the E_a value is concerned. In particular, considering the very many results on the role of oxygen doping in crystalline Si,[78] a-Si:H,[79] μc-Si:H,[80] and SIPOS[54,56] systems, and the apparent present lowering of E_a that accompanies the increase of the conductivity upon phosphorus doping in the annealed samples, we suggest that the E_a values reflect the same mechanism of the carriers activation energy in all these systems. In particular, we note that the oxygen donors in silicon are located 0.16–0.17 eV below the conduction band edge[56,81] which is very close to the E_a values that we obtained here for the annealed Si/SiO_2 undoped samples. Considering the same qualitative behavior of $\sigma(T)$ in the above systems and the above trends in the E_a values we conclude that for x removed from x_c there is no difference in the transport mechanism between systems where there may be, *a priori*, intercrystallite barriers (say, annealed films) and systems where no such barriers are expected to exist (say, nonannealed films).

After raising our doubts as to the applicability of the above simple barrier and simple hopping (see also below) models to the system that we study here we are essentially left with the interpretation of the $\sigma(T)$ dependence in terms of a variable activation energy. Such a variation can come about either from the shift of E_F through a given distribution of states[82] as is common in disordered semiconductors,[60] or it can be due to the variation of the dominant thermionic emission channel when a barrier between two crystallites exists.[25,54,56] As both types of interpretations have been proposed for SIPOS[56,82] and as SIPOS resembles most closely our samples, we consider now both of them pointing out, probably for the first time, that for dense systems of NC ensembles they amount to the same.

Our argument is as follows: for the crystallites size ($d <$ 10 nm) that we have in the present work and that Seto[25] had in his SIPOS samples, one may look at the system as if *there is no explicit space charge region surface barrier any more* but rather a simple uniform semiconductor that follows the usual carrier statistics. In that case then, as suggested by Baccarani *et al.*,[55] E_a is simply equal to E_c-E_t, where E_t is the energy of the surface states. This conclusion follows from the request of charge neutrality (i.e., from the fact that, when N_t is the *a priori* available surface states density, the density of the charge trapped in the surface states N_t' ($<N_t$) will adjust itself to become $N_t' = N_D d$ where N_D is the concentration of the donor states in the bulk of the crystallites. Hence, for small enough crystallites, if $N_D d < N_t$, there will be no potential barrier at the surface but there will be a readjustment of the Fermi level in the sample. Once this is the case, our entire ensemble of crystallites forms a bulk-like system that consists of a continuous network of crystallites with a single, well-defined E_F that is *a priori* determined by the combined state distribution of the crystallite interior and its surface. That the necessary $N_t > N_D d$ condition for that is fulfilled in our nanocrystallites is simple to see from the fact that in the annealed samples the doping is effective and thus that N_D (due to intentional and nonintentional doping) is no more than 10^{18} cm^{-3} which corresponds (for the $d \leqslant 10$ nm range) to $N_D d \leqslant 10^{12}$ cm^{-2}. On the other hand, we note that this 10^{12} cm^{-2} value is rather the lower-limit estimate of N_t in SIPOS.[25] Another argument for the applicability of the present "network" model to our NC's (in the $N_t > N_D d$ range) is the agreement of our $\sigma(N_D)$ results with those of Seto's-SIPOS[25] for N_D in the 10^{15}–10^{18} cm^{-3} range. In fact, we found in our doped Si/SiO_2 samples that the results obtained were much the same for the n and p dopings. In particular, for the n-type samples, for which we utilized 20–30 Ω cm (corresponding to $N_D \approx 10^{15}$ cm^{-3}), 0.15 Ω cm (corresponding to $N_D \approx 10^{17}$ cm^{-3}) and 0.005 Ω cm (corresponding to $N_D \approx 10^{18}$ cm^{-3}) crystalline Si wafer targets, we found that while in the nonannealed samples the *conductivities were independent of the doping,* for the annealed samples the results were very different. For example, at $x/x_c = 1.30$ the observed respective conductivities were 10^{-6}, 10^{-5}, and 10^{-3} $(\Omega\ \text{cm})^{-1}$. This similarity with Seto's data[25] further shows that the latter system is very similar to the SIPOS systems in the $N_t \geqslant N_D d$ regime.

Moreover, we note that for the crystallites sizes involved and their density, the concentration of donors (say, of the order of 10^{18} cm^{-3}) amounts to a single free electron per crystallite and thus the concept of a double Schottky-like (semiconductor-semiconductor) space charge barrier[9] becomes meaningless. Correspondingly, we argue that one cannot describe the conduction mechanism in the system that we study as reflecting thermionic emission, but rather as reflecting transport in a disordered network. *The important new point here* is then that, in the case of small enough crystallites, there is no way to distinguish between the model of a single carrier excited in a semiconductor, where E_F is determined by the density of states (DOS) distribution in the bulk and the Seto,[25] or the other, more detailed models of thermionic emission.[54,55] We note in passing that while in those works the emphasis was on the variation of N_D, in our present work, following our interest in the quantum confinement regime,[31,40] *the emphasis is on the crystallites size d*. In other words, the condition $N_t = N_D d$ marks the transition between the behavior of a barrier model and the behavior of the E_F shift within the corresponding landscape of the DOS distribution.[83]

Indeed the interpretation of $\sigma(T)$ in SIPOS in terms of a model of a disordered semiconductor bulk with a concave $\sigma(T)$ behavior was given by Hamasaki *et al.* already in 1977.[82] However, this was done without the consideration of the surface-bulk relation that we suggest here. Still, as Hamasaki *et al.*, the model we suggest is based on a continuous states distribution in the "mobility gap" and not on the presence of semiconductor barriers. Our picture of thermal excitation from band tail states to the conduction band (when these states

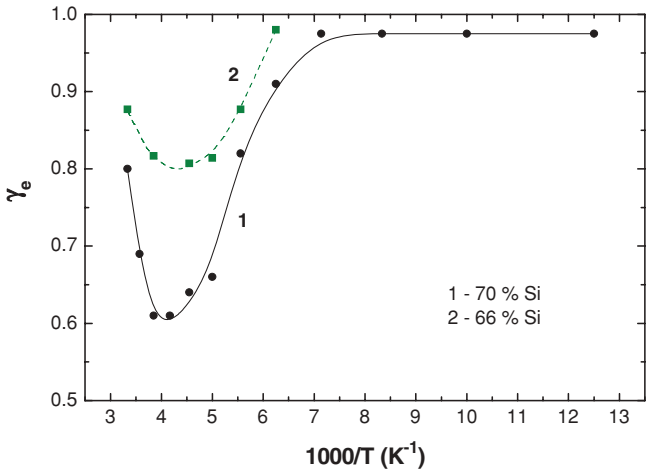

FIG. 5. (Color online) Typical temperature dependence of the light intensity exponent for samples of $x = 70$ and 66 vol.%. The curves shown are the best fits to the data. The structure of the samples on which these data were obtained is similar to the one shown in Fig. 2. These results are very similar to those obtained for μc-Si:H.

have a continuous distribution in their energies) is further supported by the photoconductivity data that we presented in Fig. 3(a). This is since the corresponding dependence is similar to the behavior observed in many works on μc-Si:H,[53,61] and thus the σ_{ph}(T) can be simply interpreted as due to the temperature induced shift of the demarcation level within the tail-like continuous state distribution in the macroscopic system.[49] In the case of μc-Si:H we have carried out a comprehensive study[53] that has shown that dependencies such as those presented here for σ_{ph}(T) in Fig. 3(a) and for γ_e(T) in Fig. 5, are conclusively associated with band tails, and that these tails are different from those that we found in a-Si:H.[44] Indeed, the simplest model of the γ_e(T) dependence follows the relation $\gamma_e(T) = T_0/(T_0 + T)$, where k$T_0$ is the width of the tail.[43] On the other hand, the behavior of σ(T) suggests that under illumination (as does E_F) the quasi-Fermi level, E_{Fq}, shifts down with increasing T. The initial decrease of γ_e(T) that is followed by its increase with increasing T in Fig. 5 is explained then as due to the fact that, at low T, E_{Fq} scans the "steeper" part of the band tail, that is close to E_c, and at higher temperatures it scans the deeper-wider part of the band tail.[82] We note in passing that other mechanisms that can account for a behavior such as we show in Fig. 5 were suggested for other systems previously.[84,85] The important point, however, is that the feature of a continuous distribution of states in the pseudo gap is common to all of them. Correspondingly, we speculate that the increase of γ_e with decreasing x, as shown in Fig. 5, is due to the increased recombination as the network become sparse due to the increase in the concentration of the total NC's surface area and thus the density of the "surface" states. This speculation is further supported by our finding that the γ_e values increase with the decrease of the illumination wavelength (437 nm instead of 628 nm) as to be expected from the enhanced light absorption at the surface and thus with the enhanced surface recombination.[9] The fact that with increasing doping we get an enhancement of σ_{ph} is also consistent with our above suggestion since E_{Fq} is closer then to E_c (i.e., the doping shifts the E_{Fq} level upward in a landscape of a continuous distribution of states).[86]

We suggest then, in the spirit of Hamasaki *et al.*,[82] that the σ(T) behavior that we observe is simply a reflection of the E_F shift within the "landscape" of a continuous distribution of states[83] that are present in the crystallites due to disorder and doping (mainly oxygen donors and acceptors). Our model accounts also for the low conductivity in the network of the touching NC's in comparison with that of the crystalline Si bulk by viewing the interface regions between the crystallites (see Figs. 1 and 2) as a source of carrier scattering. The essentials of this model were given previously by Tarng[54] for polycrystalline Si by considering the quantum mechanical reflection and the relatively low tunneling transmission through these interfaces, even for rather narrow "mismatched" barriers such as those that we see between touching NC's in Fig. 1.

Turning to the $x \approx x_c$ regime we recall that we have previously shown[30] that the $\sigma(x)$ dependence is in excellent agreement with the predictions of the critical behavior of percolation theory.[46,47,49] However, in view of the various hopping behaviors that were suggested for systems of Si NC's embedded in SiO_2[15,87] we turned to check whether this $\sigma(x)$ dependence can also be interpreted in terms of inter-NC's hopping in this regime. The predicted dependence in this case is based on the expectation that the interparticle tunneling route will prefer the nearest neighbors that correspond to the average lowest-tunneling resistance that enables a continuous percolation path. In that (critical path) hopping-like case one can further show that $\sigma \propto \exp(-\alpha x^{-1/3})$, where, α is a known constant.[48,49] This dependence applies in the dilute (low-x) limit and can be easily shown[49,88,89] to become of the form $\sigma(x) \propto \exp(-\alpha' x^{-1})$ (where the constant α' is replacing the constant α) in the denser (higher-x) ensembles case. As seen in Fig. 6 the data cannot be fitted by the previous given hopping-like dependencies.[49,88] In contrast, we found (following our well-checked fitting procedure)[30,90] that these results are well characterized by the percolation $\sigma \propto (x\text{-}x_c)^t$ dependence (here with $x_c = 31$ vol.% and $t = 2.5$) and that the value of t is independent of temperature.[89] These observations lend then further support for the "coalescence" scenario, in contrast with the VRH scenario in the $x \geqslant x_c$ regimes.

Following the previous percolation scenario that appears to describe well the system around x_c let us discuss now in more detail the interparticle process that controls the transport via the percolation network. We can expect that upon approaching the percolation threshold from above (i.e., by lowering the value of x toward x_c) we will find some geometrically isolated NC's that are critical in the electrical network. Such single particle "bottlenecks" are expected to show a DBTJ behavior.[30] That this situation is geometrically likely is illustrated by the bright (yellow) segments in Fig. 2. Also, electrically, such "nontouching" single NC's are expected to show local charging effects.[10] The fulfillment of this expectation is exhibited by the temperature-dependent normalized I-V characteristics that are shown in Fig. 7. These characteristics that were taken at a bias scan rate of 0.07 V/sec differ from those of slow (less than 0.01 V/sec) scans[30] by exhibiting a temperature-dependent hysteresis. The "flat"-horizontal portions of the I-V's that are exhibited in Fig. 7 are the "split" parts of the voltage gap[30] that become less and less apparent as the temperature

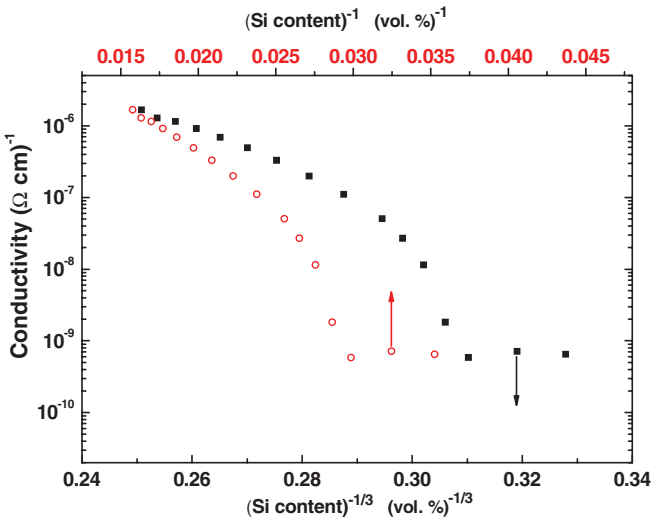

FIG. 6. (Color online) A typical $\sigma(x)$ characteristic when presented on a $x^{-1/3}$ (solid squares) and a x^{-1} (open circles) scales. The lack of linearity in the scales shown indicates that for the $x > x_c$ regime the conductivity cannot be accounted for by intercrystallite hopping. On the other hand, these data are well presented by the expected percolation behavior, yielding a percolation threshold x_c of 31 vol.% and a critical exponent of 2.5.

decreases due to the corresponding larger "RC" time. We note here that, as with increasing temperature, the lowering of the scan rate (in the 1 V/sec to 0.02 V/sec range) has the same effect, that is, the hysteresis ceases and the voltage gap split decreases until the corresponding voltage gap segments "unite" around the (I = 0, V = 0) origin. All these phenomena are apparent for x values in the close vicinity of x_c but they do not appear to exist away ($x > x_c = 37$ vol.% here) from this vicinity. These findings clearly indicate that there is a stored charge in the continuous network that tends to discharge with time, and that this discharge is accelerated with increasing

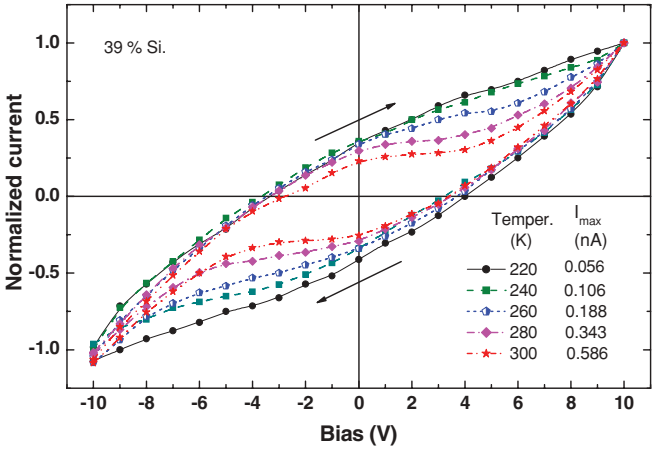

FIG. 7. (Color online) (a) The measured normalized (each by its I_{max}) I-V characteristics as obtained, under a bias scan of 0.07 V/sec, for a sample in the close vicinity ($x = 39$ vol.%) of the percolation threshold (here $x_c = 37$ vol.%). The hysteresis "shrinks" and the "voltage gap" is more pronounced as the temperature is increased. Very similar I-V characteristics were obtained for the photocurrents.

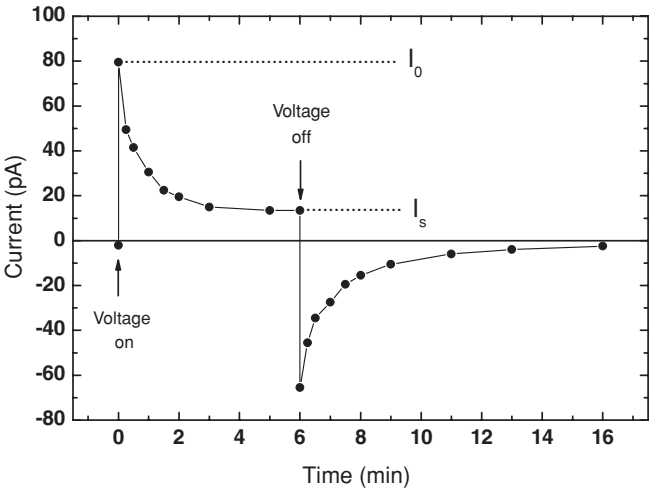

FIG. 8. A typical I-t characteristic as obtained for a sample in the very close vicinity of x_c ($x = 37.7$ vol.%), under the application of a bias of 5 V. Note that there is evidence by the current decay and the response to switching for substantial charge storage. This behavior is obtained only in the close vicinity of x_c. The initial current I_0 and the steady-state current I_s are indicated in the figure. The estimated stored charge was derived from such data by considering the area under the current decay curves between I_0 and I_s or by applying the Wagner-circuit model that consists of a resistor R_s that is connected in series with a parallel configuration of a resistor R_p and a capacitor C_e.

temperature. Another manifestation of the charging effect is exhibited in Fig. 8, where we show the I-t characteristics in the close vicinity of the percolation threshold. As shown in this figure, both the application and the removal of the voltage are accompanied by a current decay and there is an inversion of the current sign in the latter case. Again, this behavior is typical only of the close vicinity of x_c. For $x > x_c$ (say, $x =$ 60 vol.%) no such charging or discharging effects are found within the (1 s) resolution of the present measurements. In this figure we denoted the initial and the steady-state currents between adjacent electrodes by I_0 and I_s, respectively.

To confirm that charging effects are responsible for the results shown in Figs. 7 and 8 and to quantitatively determine the stored charge we have measured (with an applied voltage of 5 V) both, a hysteretic I-V characteristic, such as in Fig. 7, and an I-t characteristic such as in Fig. 8. The value of the stored charge Q in the latter case can be approximated in two simple ways. The simplest one is finding the "area" $Q = \int [\mathrm{I(t)}\text{-}I_s]dt$ following the bias application or the "area" $Q = \int I(t)dt$ following the termination of the bias. The other approach is to consider the above I_0 and I_s values and using then the simplest equivalent circuit that captures the essence of the system (i.e., the so-called Wagner circuit).[91] This circuit consists of a resistor R_s that is connected in a series with a parallel connection of a resistor R_p and a capacitor C_e. We note, of course, that the value of C_e reflects some macroscopic average of the microscopic details. In the present work this must yield a much larger value than the simple geometrical capacitance of the sample between the two electrodes in our coplanar configuration (which is of the order of 10^{-15} F). The charging or discharging time of such a circuit is simply given by

$\tau = C_e R_s R_p/(R_s + R_p)$ and the current dependence on time is given then by $I(t) = V_o\{1/(R_s + R_p) + [1/R_s\text{-}(1/(R_s + R_p)]\exp(-t/\tau)\}$ where V_o is the applied bias at $t = 0$. Determining the parameters of the latter equation from the experimental $I(t)$ dependence and applying again the simple $Q = \int [I(t)\text{-}I_s]dt$ relation gives then the estimated value of the charge. We have also modeled the hysteretic behavior, shown in Fig. 7, by the Wagner circuit,[91] however, the corresponding formulation of the analysis is somewhat long and will not be given here.

The results of all the analyses mentioned previously yielded Q values that were in agreement with those derived for the corresponding x value in our previous capacitance-voltage (C-V) data for the same applied bias.[31] In particular, all of them indicated that the stored charge is of the order of 3 nC, which corresponds to about 5×10^{15} cm^{-3} elementary charges in the coplanar configuration of our samples. One should note, of course, that this means that at the $x \approx x_c$ regime, less than 1% of the crystallites in the system are charged. In turn, this finding supports our conjecture that, in practice, only the single-individual, nontouching, NC's retain their charge, on the one hand, and the existence of DBTJ's in this regime, on the other hand. This justifies also our interpretation of the conduction path in the structural image given in Fig. 2 as indicated by the light (yellow) segments in the figure. It is interesting to note in passing that the DBTJ configuration[30] that we concluded here from a macroscopic study of the system can reproduce the DBTJ that is provided by a microscopic single-electron transistor that is fabricated by lithographic techniques.[15]

A result that further supports our model of the "local" nature of the charging effect is the dependencies of I_0 and I_s on temperature. We found, as shown in Fig. 9, that the activation energy of the charged state (I_s) is larger than that of the initial state (I_0), indicating the presence of a Coulomb blockade. In fact, the difference between the two is of the order expected[24] for a single DBTJ (here 0.05 eV). In turn, this strongly suggests

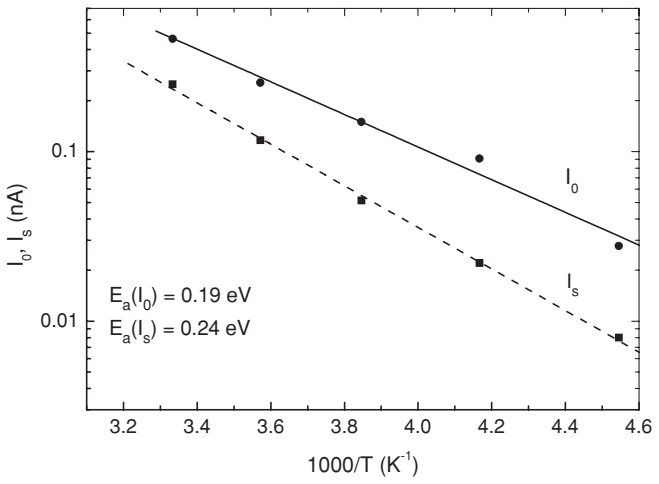

FIG. 9. The temperature dependence of the initial and steady-state currents for a sample in the very close vicinity of x_c ($x =$ 37.7 vol.%,) under the application of a bias of 20 V. Note that there is a difference in the activation energies of the two currents.

that the increase of E_a as $x \to x_c$ that we found from the $\sigma(T)$ dependence is associated with the CB effect in our samples.

IV. SUMMARY AND DISCUSSION

In this work we studied the conduction mechanism in relatively dense ensembles of Si quantum dots. Starting with the $x \approx x_c$ regime we have clearly confirmed the role of the DBTJ's by the presence of a "voltage gap," the increase of E_a as x decreases toward x_c and our quantitatively determined charging effects that are similar to those observed in lithographically fabricated single electron transistors.[15] On the other hand, from the results that we reported here we cannot estimate the relative contribution of the CB and quantum confinement. In fact, we note that as here, while the presence of charging (CB) is well established in the literature[15] for Si NC's, there is no conclusive evidence for the quantum confinement effect on the transport (i.e., the presence of resonant tunneling) in these systems. This applies even to local transport measurements, as the corresponding confinement energy values suggested from those measurements[15] have not been confirmed by other parallel (say, optical) evidence. Rather, *ad hoc*, very simple models have been suggested.[15] While our work is concerned with relatively dense ensembles of Si NC's (that are QD's, as evidenced by our optical studies)[45] it appears that our previous results on such ensembles provide a hint as to the involvement of the resonant tunneling effect. The evidence for that is the charge polarization effect that we found to be induced in a string of Si NC's with a monotonic change of the crystallites size.[41] In that work we revealed an anomalous photovoltaic phenomenon for x just above x_c. We interpreted that observation to be due to the interplay between the quantum confinement and the CB effects within clusters of Si NC's.[41] Very recently we have found further support for that interpretation by observing that the maximum of the effect shifts to smaller crystallites when the excited photon energy is blue shifted, indicating that the effect is associated indeed with the size of the participating crystallites.

Turning to the connectivity of the system, just above the observed percolation threshold, we have enough of the adjacent Si NC's that "touch" their neighbors and thus the dominant current takes place via a percolation network of "touching" NC's. This conclusion is based on the percolation dependencies of both $\sigma(x)$ and $\sigma_{ph}(x)$ and the structural results that we have found in our previous studies[30] and here. In fact, this percolation-like behavior is a confirmation of a suggestion made previously for μc-Si:H[92] that the photogenerated carriers that contribute to the photoconductivity are only those that are generated in the backbone of the corresponding percolation network (i.e., in the network that we attribute here to consist of touching crystallites). We note, however, that, *a priori*, in ensembles of conducting particles two types of percolation transitions are possible in principle. In the first type, the conduction above the corresponding percolation transition is of the tunneling-percolation type[47,49] while in the other type the conduction is associated with a network of coalescing grains.[7,8,52,88] We concluded that for the system of $x > x_c$, that we study here, there is strong supporting evidence only for the second type of transition except that instead of a coalescence

of the metallic grains (as in granular metals) we have here the touching between the NC's. This conclusion follows the "visible" touching that we have observed in the HRTEM images, and the observation of a percolation behavior with a t and x_c values that are both independent of temperature.[89] Also, the observation that the x_c values of the thresholds that we found here are between that of the effective medium (EM) value (of a fractional conducting phase content of 33 vol.%)[48] and the ($\sim$50 vol.%) values[33,52] that are typical of granular metals lend additional support for our view of the conducting network.

Establishing the connectivity of the system we turn to the evaluation of the interparticle transport mechanism. The four conspicuous mechanisms that may, in principle, account for our observed σ(T) dependence are (i) thermionic emission over barriers between adjacent semiconductor crystallites,[15,25] (ii) thermally activated tunneling,[69,72] (iii) versions of variable range or near-neighbor hopping,[36,63] and (iv) temperature-induced shift of E_F throughout a landscape of the state distribution in the mobility gap (similar to the one suggested for the E_F shift via the band tails of a-Si:H[83] and μc-Si:H[93,94] systems). The main effort in the present work was to decide which of the four mechanisms is the most likely one for the system under study in the $x \geqslant x_c$ regime. This effort concentrated on the measurement and analysis of the observed σ(T) and σ_{ph}(T) characteristics on the various sputtered systems that we studied (some with possible potential barriers and some without such barriers). In particular, our study enabled us to exclude the two most "popular" mechanisms suggested previously[15] for the transport in dense ensembles of Si NC's. These are the hopping between crystallites and the thermionic emission processes.

The physics revealed in the consideration of the latter mechanism is quite interesting. In particular, we have presented three main reasons for the conclusion that the semiconductor-semiconductor-barrier-based models do not apply to the present system of Si NC's. The first is that the observed dependencies of σ(T) and σ_{ph}(T) are very similar to those observed not only in various microcrystalline[95] and nanocrystalline[26] Si materials, but also in a-Si:H[96–98] where there *are no apparent barriers in the system*. The second reason is that the "double" Schottky barrier-like depletion region that is needed for the fulfillment of the thermionic emission models[25,54,56] cannot be applied to the systems studied here due to the very few donors (or charges) that may be introduced into a single NC. The third reason is that the distinction between the surface and bulk states becomes blurred[55] as the crystallite size becomes less than 10 nm. Correspondingly, we suggested that the narrow separation between touching crystallites acts "only" as a local disturbance in the potential landscape over distances that are of the order of the size of the NC's. This view is supported by the closely related system of μc-Si:H for which there is ample evidence against the role of the intercrystallite barriers from the estimations of their small heights,[99,100] small widths,[26,101] and negligible effect on the transport.[102] This picture is also consistent with the relatively high mobility values (>1 cm^2/Vsec) that were determined for μc-Si:H structures.[94,102,103] We conclude then that the interfaces between the NC's provide "minor" (low and narrow) potential barriers that act more like scattering centers (e.g., by quantum reflections and/or disturbing local atomic potentials)[56] than surmountable barriers. Hence, we suggest that the latter potential fluctuations are similar to those of defects in crystals or imperfections in disordered semiconductors.

The picture that we propose then is that in the high-x ($>x_c$) regime we have a continuous disordered network through which the carriers propagate under the effect of potential fluctuations, and that these, as outlined theoretically by O'Leary and Lim,[104] are manifested by a band tail state distribution that is reminiscent of (but different in detail from) the Cohen, Fritzsche, and Ovshinsky (CFO) model.[105] A strong support to our view comes also from the similarity of the photoconductivity behavior found here for ensembles of Si NC's and a-Si and the behavior found in a-Si:H[86,106] and disordered chalcogenides.[43] In particular, we found a γ_e(T) behavior that we have shown previously to be associated with recombination in band tails.[53] The major conclusion of this paper is then that our findings for the transport in the $x > x_c$ regime are consistent with the model of the temperature-induced shift of the Fermi level within the DOS of a disordered semiconductor, in general, and in a band-tail states landscape, in particular.[83,96,102] In principle, this was also the view of Hamasaki *et al.*[82] in their interpretation of the temperature dependence of the conductivity in SIPOS which is a Si/SiO_2 system that is quite similar to that of ours. Adopting the previous model, we suggest then that the activation energy derived at a given temperature reflects (but is not necessarily equal to) the E_c-E_F separation (where E_c here is the mobility edge of the conduction band). Consistent with our results, the effect of doping was then to reduce the values of E_c-E_F and E_c-E_{Fq} for a given landscape of the DOS. Following the above we also suggest that at the very low temperatures the hopping in the $x > x_c$ regime is not between the crystallites, as proposed for the $x < x_c$, regime,[28,29] but between the defect states that exist in the NC's, their surfaces and/or the boundaries between them when they touch. The above conclusion is based on the fact that hopping phenomena become significant only at low ($T < 50$ K) temperatures[60,61] and the fact that there is very little evidence in the literature to support the existence of the various hopping mechanisms in the temperature range studied here.

In conclusion, in this work we studied the transport mechanism of relatively high-density Si NC's ensembles that are embedded in an insulating matrix. We found that while tunneling conduction and CB effects exist in the percolation threshold end of that regime, for higher densities the electrical transport is determined by a continuous global network such as the one encountered in bulk disordered semiconductors.

ACKNOWLEDGMENTS

This work was supported, in part, by the Israel Science Foundation (ISF) and, in part, by the German Ministry for the Environment, Nature Conservation, and Nuclear Safety. The authors would like to thank M. I. Alonso, I. V. Antonova, Y. Goldstein, O. Millo, A. G. Nassiopoulou, and A. Sa'ar for their valuable contribution to the work reported here. I.B. acknowledges the support of the Enrique Berman chair of Solar Energy Research at the Hebrew University.

[1] S. V. Gaponenko, *Optical Properties of Semiconductor Nanocrystals* (Cambridge University Press, Cambridge, 1998).

[2] I. Balberg, E. Savir, Y. Dover, O. Portillo-Moreno, R. Lozada-Morales, and O. Zelaya-Angel, Phys. Rev. B **75**, 153301 (2007).

[3] For a review see O. Bissi, S. Ossicini, and L. Pavesi, Surf. Sci. Rep. **38**, 1 (2000).

[4] I. Balberg, J. Nanoscience and Nanotechnology **8**, 745 (2008).

[5] A. Nissiopoulou, in *Encyclopedia of Nanoscience and Nanotechnology* (American Scientific, Vlencia, CA, 2004), Vol. 9, p. 793.

[6] A. Kolek, J. Phys. Condens. Matter **6**, 469 (1994).

[7] B. Abeles, P. Sheng, M. D. Coutts, and Y. Arie, Adv. Phys. **24**, 407 (1975).

[8] B. Abeles, in *Applied Solid State Science*, 6 (Academic Press, New York, 1976), p. 1.

[9] S. M. Sze and K. K. Ng, *Physics of Semiconductor Devices* (Wiley, Hoboken, NJ, 2007).

[10] *Single Electron Tunneling*, edited by H. Grabert and M. H. Devoret, (Plenum, New York, 1991).

[11] C. A. Stafford and S. Das Sarma, Phys Rev. Lett. **72**, 3590 (1994).

[12] S.-K. Kim, C.-H. Cho, B.-H. Kim, S.-J. Park, and J. W. Lee, Appl. Phys. Lett. **95**, 143120 (2009).

[13] N. Daldosso and L. Pavesi, *Low Dimensional Silicon as a Photonic Material, in Nanosilicon*, edited by V. Kumar (Elsevier, Amsterdam, 2008), p. 314.

[14] T. A. Burr, A. A. Seraphin, E. Werwa, and K. D. Kolenbrander, Phys. Rev. B **56**, 4818 (1997).

[15] For reviews see Z. A. K. Durrani and H. Ahemed, *Nanosilicon Single-Electron Transistors and Memory, in Nanosilicon*, edited by V. Kumar (Elsevier, Amsterdam, 2008), p. 335 and I. Antonova, *Electrical Properties of Semi-Conductor Nanocrystals and Quantum Dots in Delectric Matrix, in Nanocrystals and Quantum Dots of Group IV Semiconductors*, edited by T.V. Torchynska and Yu. V. Vorobiev (ASP, Stevenson Ranch, CA, 2009).

[16] S. Y. Ren and J. D. Dow, Phys. Rev. B **45**, 6492 (1992).

[17] M. Mahdouani, R. Bourguiga, and S. Jaziri, Physica E **41**, 228 (2008).

[18] N. A. Hill and K. B. Whaley, Phys. Rev. Lett. **75**, 1130 (1995).

[19] O. Millo, D. Katz, Y.-W. Cao, and U. Banin, Phys. Rev. Lett. **86**, 5751 (2001).

[20] D. L. Klein, R. Roth, A. K. L. Lim, A. P. Alvisatos, and P. L. McEuen, Nature (London) **389**, 699 (1997).

[21] M. Fujii, O. Mamezaki, S. Hayashi, and K. Yamomoto, J. Appl. Phys. **83**, 1507 (1998).

[22] M. A. Rafiq, Y. Tsuchiya, H. Mizuta, S. Oda, S. Uno, Z. A. K. Durnani, and W. I. Milne, J. Appl. Phys. **100**, 014303 (2006).

[23] X. Zhou, K. Usami, M. A. Rafiq, Y. Tsuchiya, H. Mizuta, and S. Oda, J. Appl. Phys. **104**, 024518 (2008).

[24] S. Huang, S. Banerjee, R. T. Tung, and S. Oda, J. Appl. Phys. **94**, 7261 (2003).

[25] J. Y. W. Seto, J. Appl. Phys. **46**, 5247 (1975).

[26] Y. He, Y. Wei, G. Zheng, M. Yu, and M. Liu, J. Appl. Phys. **82**, 3408 (1997).

[27] K. Nishiguchi and S. Oda, J. Appl. Phys. **88**, 4186 (2000).

[28] P. Sheng and J. Klafter, Phys. Rev. B **27**, 2583 (1983).

[29] E. Simanek, Solid State Commun. **40**, 1021 (1981).

[30] I. Balberg, E. Savir, J. Jedrzejewski, A. G. Nassiopoulou, and S. Gardelis, Phys. Rev. B **75**, 235329 (2007).

[31] I. V. Antonova, M. Gulyaev, E. Savir, J. Jedrzejewski, and I. Balberg, Phys. Rev. B **77**, 125318 (2008).

[32] J. J. Hanak, J. Mater. Sci. **5**, 964 (1970).

[33] B. Abeles, H. L. Pinch, and J. I. Gittleman, Phys. Rev. Lett. **35**, 247 (1975).

[34] N. Karpov, V. Volodin, J. Jedrzejewski, E. Savir, I. Balberg, Y. Goldstein, T. Egewskaya, N. Shwartz, and Z. Yanovitskaya, J. Optoelecrtonics and Advanced Materials **11**, 625 (2009).

[35] I. V. Antonova, M. Gulyaev, Z. Sh. Yanovitskaya, V. A. Valodin, D. V. Marin, M. D. Efremov, Y. Goldstein, and J. Jedrzejewski, Semiconductors **40**, 1198 (2006).

[36] M. Fujii, Y. Inoue, S. Hayashi, and K. Yamamoto, Appl. Phys. Lett. **68**, 3749 (1996).

[37] For a review of the structural and optical properties of our samples, see A. Sa'ar, J. Nanophotonics **3**, 032501 (2009).

[38] M. Dovrat, Y. Goshen, I. Popov, J. Jedrzejewski, I. Balberg, and A. Sa'ar, Phys. Stat. Sol. (c) **2**, 3440 (2005).

[39] A. Sa'ar, Y. Reichman, M. Dovrat, D. Kraf, J. Jedrzejewski, and I. Balberg, Nano Lett. **5**, 2443 (2005).

[40] M. Dovrat, Y. Goshen, J. Jedrzejewski, I. Balberg, and A. Sa'ar, Phys. Rev. B **69**, 155311 (2004).

[41] H. Levi Aharoni, D. Azulay, O. Millo, and I. Balberg, Appl. Phys. Lett. **92**, 112109 (2008) and unpublished.

[42] See, for example, D. Azulay, I. Balberg, V. Chu, J. P. Conde, and O. Millo, Phys. Rev. B **71**, 113304 (2005).

[43] R. H. Bube, *Photoelectronic Properties of Semiconductors* (Cambridge University Press, Cambridge, England, 1992).

[44] I. Balberg, R. Naidis, L. F. Fonseca, S. Z. Weisz, J. P. Conde, P. Alpuim, and V. Chu, Phys. Rev. B **63**, 113201 (2001).

[45] M. I. Alonso, I. C. Marcus, M. Garriga, and A. R. Goñi, J. Jedrzejewski, and I. Balberg, Phys. Rev. B **82**, 045302 (2010).

[46] D. Stauffer and A. Aharony, *Introduction to Percolation Theory* (Taylor and Francis, London, 1994).

[47] I. Balberg, *Continuum Percolation*, *in Springer Encyclopedia of Complexity*, 2, edited by M. Sahimi (Springer, Berlin, 2009), p. 1443.

[48] B. I. Shklovskii and A. L. Efros, *Electronic Properties of Doped Semiconductors* (Springer-Verlag, Berlin, 1984).

[49] I. Balberg, J. Phys. D Appl. Phys. **42**, 064003 (2008).

[50] I. Balberg, Phys. Stat. Sol. (c) **5**, 3771 (2008).

[51] N. F. Mott and E. A. Davis, *Electron Processes in Non-crystalline Materials* (Clarendon, Oxford, 1979).

[52] I. Balberg, D. Azulay, D. Toker, and O. Millo, Int. J. Mod. Phys. B **18**, 2091 (2004).

[53] I. Balberg, Y. Dover, R. Naides, J. P. Conde, and V. Chu, Phys. Rev. B **69**, 035203 (2004), and references therein.

[54] M. L. Tarng, J. Appl. Phys. **49**, 4069 (1978).

[55] G. Baccarani, B. Ricco, and G. Spadini, J. Appl. Phys. **49**, 5565 (1978).

[56] S. Lombardo, S. U. Campisano, and F. Baroetto, Phys. Rev. B **47**, 13561 (1993).

[57] A. H. Clark, Phys. Rev. **154**, 750 (1967).

[58] A. Lewis, Phys. Rev. Lett. **29**, 1555 (1972).

[59] S. J. Bending and M. R. Beasley, Phys. Rev. Lett. **55**, 324 (1985).

[60] S. R. Elliott, *Physics of Amorphous Materials* (Longman, New York, 1990).

[61] J.-H. Zhou, S.D. Baranovski, S. Yamasaki, K. Ikuta, K. Tanaka, M. Kondo, A. Matsuda, and P. Thomas, Phys. Stat. Sol. (b) **205**, 147 (1998).

[62] A. J. Houtepen, D. Kockmann, and D. Vanmaekelbergh, Nano Lett. **8**, 3516 (2008).

[63]S. Banerjee, Physica E **15**, 164 (2002).
[64]M. Berthelot, Ann. Chim. Phys. **66**, 110 (1862).
[65]J. J. Mares, J. Kristofik, and V. Smid, Semicond. Sci. Tecnol. **7**, 119 (1992).
[66]R. A. Street, Adv. Phys. **25**, 397 (1976).
[67]J. J. Mares, J. Kristofik, J. Pangrac, and A. Haspodkova, Appl. Phys. Lett. **63**, 180 (1993).
[68]D. R. Stewart, D. A. A. Ohlberg, P. A. Beck, C. N. Lau, and R. Stanley Williams, Appl. Phys. A **80**, 1379 (2005).
[69]M. Kapoor, V. A. Singh, and G. K. Johri, Phys. Rev. B **61**, 1941 (2000).
[70]B. Fisher, K. B. Chashka, L. Patlagan, and G. M. Reisner, Phys. Rev. B **70**, 205109 (2004).
[71]S. J. Konezny, M. N. Bussac, and L. Zuppiroli, Appl. Phys. Lett. **92**, 012107 (2008).
[72]P. Sheng, E. K. Sichel, and J. I. Gittleman, Phys. Rev. Lett. **40**, 1 (1978).
[73]J. H. Werner, Solid State Phemon. **37-38**, 213 (1994).
[74]L. I. Glazman and K. A. Matveev, Sov. Phys. JETP **67**, 1276 (1988).
[75]A. I. Yakimov, N. P. Stepina, and A. V. Dvurechenskii, J. Phys. Condens. Matter **6**, 2583 (1994).
[76]D. Popovic, A. B. Fowler, and S. Washburn, Phys. Rev. Lett. **67**, 2870 (1991).
[77]H. F. Wolf, *Semiconductors* (Wiley-Interscience, New York, 1971).
[78]P. Morgen, U. Hofer, W. Wurth, and E. Umbach, Phys. Rev. B **39**, 3720 (1989).
[79]K. Winer, J. Vac. Sci. Technol. B **7**, 1226 (1989).
[80]T. Kamei and T. Wada, J. Appl. Phys. **96**, 2087 (2004).
[81]V. N. Mordkovich, Sov. Phys.-Solid State **6**, 654 (1964).)
[82]M. Hamasaki, T. Adachi, S. Wakayama, and M. Kikuchi, Solid State Comun. **21**, 591 (1977).
[83]H. Overhof and P. Thomas, *Electron Transport in Hydrogenated Amorphous Silicon* (Springer-Verlag, Berlin, 1989).
[84]F. T. Reis and I. Chambouleyron, J. Non-Cryst. Solids **299**, 179 (2002).
[85]C. Main, F. Dick, S. Reynolds, W. Gao, and R. A. G. Gibson, J. Non-Cryst. Solids **200**, 263 (1996).
[86]H. Fritzsche, B.-G. Yoon, D.-Z. Chi, and M. Q. Tran, J. Non-Cryst. Solids **141**, 123 (1992).
[87]T. Wang, W. Wei, G. Xu, and C. Zhang, Int. J. Mod. Phys. B **16**, 4289 (2002).
[88]G. Ambrosetti, C. Grimaldi, I. Balberg, T. Maeder, A. Danani, and P. Ryser, Phys. Rev. B **81**, 155434 (2010); G. Ambrosetti, I. Balberg, and C. Grimaldi, Phys. Rev. B **82**, 134201 (2010).
[89]I. Balberg, G. Ambrosetti, and C. Grimaldi (unpublished).
[90]Z. Rubin, S. A. Sunshine, M. B. Heaney, I. Bloom, and I. Balberg, Phys. Rev. B **59**, 12196 (1999).
[91]B. Gross and M. T. de Figueiredo, J. Phys. D Appl. Phys. **18**, 617 (1995).
[92]F. Siebke, S. Yato, Y. Hishikawa, and M. Tanaka, J. Non-Cryst. Solids **227**, 977 (1998).
[93]M. Mars, M. Fathallah, E. Tresso, and S. Fenero, J. Non-Cryst. Solids **299**, 133 (2002).
[94]C. E. Nebel, M. Rother, M. Stutzmann, C. Summonte, and M. Heintze, Phil. Mag. Lett. **74**, 455 (1996).
[95]N. Pinto, M. Ficcadenti, L. Morresi, R. Murri, G. Ambrosone, and U. Coscia, J. Appl. Phys. **96**, 7306 (2004).
[96]K. Shimakawa and A. Ganjoo, Phys. Rev. B **65**, 165213 (2002).
[97]N. Lustig and W. E. Howard, Solid State Commun. **72**, 59 (1989).
[98]I. P. Zvyagin, I. A. Kurova, M. A. Nal'gieva, and N. N. Ormont, Semiconductors **40**, 108 (2006).
[99]A. Heya, A.-Q. He, N. Otsuka, and H. Matsumura, J. Non-Cryst. Solids **227–230**, 1016 (1998).
[100]Y. Furuta, H. Mizuta, K. Nakazato, T. T. Yong, T. Kamiya, Z. Durrani, H. Ahmed, and K. Taniguchi, Jpn. J. Appl. Phys. **40**, L615 (2001).
[101]F. Diehl, M. Scheib, B. Schroder, and H. Oechsner, J. Non-Cryst. Solids **227**, 973 (1998).
[102]D. Ruff, H. Mell, L. Toth, I. Sieber, and W. Fuhs, J. Non-Cryst. Solids **230**, 1011 (1998).
[103]T. Dylla, F. Finger, and E. A. Schiff, Appl. Phys. Lett. **87**, 032103 (2005).
[104]S. K. O'Leary and P. K. Lim, Solid State Commun. **101**, 513 (1997).
[105]H. Cohen, H. Fritzsche, and S. R. Ovshinsky, Phys. Rev. Lett. **22**, 1065 (1969).
[106]L. Fonseca, S. Z. Weisz, R. Rapaport, and I. Balberg, Mater. Res. Soc. Symp. Proc. **557**, 439 (1999).